

## Numerical Simulation of Heat Transfer during Solidification of Al–Cu Alloy Ingots Cast in a Cylindrical Mold for Different Conditions

**Farouk M. Mahdi <sup>a</sup>, Sami R. Aslan <sup>b</sup>, Mahmud H. Ali <sup>c,\*</sup>**

<sup>a</sup> Department of Mechanical Engineering, College of Engineering, Tikrit University, Tikrit, Iraq

<sup>b</sup> Electronic and Control Engineering Technology, Technical College Kirkuk, Kirkuk, Iraq

<sup>c</sup> Department of Mechanical Engineering, College of Engineering, Kirkuk University, Kirkuk, Iraq

---

### Abstract

In this paper, two dimensional numerical simulation of heat transfer during solidification of Al- 4.5 wt. % Cu alloy cast in a cylindrical mold was carried out to specify the optimum solidification conditions. The mold has the dimensions of 150 mm height, 38 mm outer radius, and 8 mm thickness. Four cases were studied for the solidification process; first case is the solidification in the mold without applying any thermal effects at four different mold temperatures of 25, 50, 100 and 200 °C respectively. The second case is insulating the cast from the top. The third case is insulating the upper portion of the mold wall. The last case is adding heat to the upper portion of the mold wall for specific time. For the last three cases, the mold temperature is set to 25°C. The results have shown that the increase in mold temperature only increases the solidification time and it does not significantly affect the temperature distribution and the final cast shape. Insulating the top of the mold made the last solidification region to be at the top of the cast, which leads to get ingot free from the secondary cavity. Insulating a portion of the upper wall of the mold made the cast surface to be more homogeneous with smallest secondary cavity. Heat addition to a portion of the upper wall of the mold leads to obtain a cast with approximately flat surface that is free from secondary cavity in addition to the primary cavity.

**Keywords:** Al 4.5 wt. % Cu alloy ingot casting; heat transfer; numerical simulation; cylindrical metal mold.

### 1. Introduction

Casting is one of the oldest crafts practiced by humans and it is one of the most important manufacturing operations. Numerous engineering industries still depend on the casting process in spite of the great development of other manufacturing processes. Casting has many advantages due to its economical nature that can be used in ferrous and nonferrous metals and to produce complex shapes with very big or very small sizes [1],[2]. The process of casting involves making cavity for the required geometric shape (called mold) then melting the metal and pouring it into the mold cavity. The solidification of the metal starts by dissipating heat to the surrounding through the mold walls until full freezing occurs [3].

The process of metal melting and solidification is achieved by gaining and dissipating heat respectively. During melting and solidification, phase change is occurred from solid phase to liquid phase and vice versa and the process is at transient heat transfer state. The main requirement for the process of casting is the production of castings that is free of common defects such as porosity, isolation, and different kinds of cavities, or minimization these defects as much as possible. This could be achieved by good control of the solidification process [1],[2],[4]. Aluminum alloys have become widespread in industries because of several advantages such as low density (light weight), good workability, corrosion resistance, response to thermal treatment and good electrical and thermal conductivity. Hence, aluminum alloys are interested by the industrialists and researchers in order to obtain castings with no defects having good properties that can achieve the desired goal of utilization.

---

\* Corresponding author. Tel.: +964-7435569706

E-mail: mahmoud75@uokirkuk.edu.iq

© 2016 International Association for Sharing Knowledge and Sustainability

DOI: 10.5383/ijtee.13.01.009

In the work of Ferreira et al [5], solidification experiments were carried out with alloys of two metallic systems. The experimentally obtained temperatures were used numerically to determine the transient metal/mold heat transfer coefficient. Quantitative models of heat transfer coefficient through casting solidification were suggested by Bertelli et al [6], using temperatures measured for both casting and mold, along with the theoretical and numerical model in cylindrical castings.

Determination of heat transfer coefficient is essential for the researches that were carried out by Santos et al [7] and Silva et al [8]. It was obtained that the magnitude of the metal/mold heat transfer coefficient and its variation in time frequently exerts a controlling influence on the freezing conditions within the casting, particularly with molds of high heat diffusivity. The research of Spinelli [9] showed that the mechanical properties of Al alloys chill castings depend on the heat transfer coefficient through interrelations solidification thermal parameters, microstructure and tensile properties

Bermudez and Otero [10], considered an enthalpy formulation of a two-phase Stefan problem arising from the solidification of aluminum during the casting process. The numerical results were presented and compared with industrial experimental measurements. The non-linear inverse heat transfer issue was used by Abbas et al [11] to formulate the solidification control of the alloy material. The governing equations derivative by employing the enthalpy methods.

In the analysis of Shi and Guo [12], a heat transfer model was established for a continuous wire casting process with a tapered cuboid casting channel. A finite difference method was used for the numerical simulation. The effects of the processing and geometric parameters were analyzed at solidification time and position where the final solidification takes place. Kulkarni and Radhakrishna [13] presented an experimental investigation to measure the solidification time in a cylindrical hollow casting cast in CO<sub>2</sub>-Sand molds using Al-4.5%Cu alloy. The results were compared with that computed using an implicit alternating direction (IAD) method including the treatment of interracial nodes between metal and mold, and boundary nodes on the mold surface.

During the solidification process, one of the most important factors that affect the final product is the location of the last solidified region due to the problems that may arise from it, such as cracks, cavities and secondary piping. These problems can be indicated through the temperature distribution contours during the casting process. Practical methods for temperature measurement inside the cast during the solidification process are very difficult or impossible without damaging a part or whole of the casting. The appropriate method is theoretical modeling of solidification process by numerical analysis that is widely used by the researchers. This is due to the great development that has been occurring in computer technology and techniques of numerical analysis methods, which are powerful tools to simulate the physical state of the solidification process accurately to determine the best conditions for castings free from defects as much as possible. Then applying these optimized conditions to produce casting with the best state.

The objective of the present study is to simulate 2D heat transfer during solidification to study the effects of the solidification configuration on the primary and secondary cavities and specify the optimum solidification conditions for aluminum-copper Al 4.5 wt. %Cu alloy cast in a cylindrical mold. The shape and dimensions of the mold are shown schematically in Fig. 1a. This can be done by identifying the last frozen area of the alloy and trying to move it to the top of the cast and make it flat as much as possible, which is indicated by temperature distribution

counters, movement of the mushy zone and cooling curves during the process of solidification. Four different cases are studied to include the effect of the mold temperature, insulating of the mold top, thermal insulation of half of the mold sides, and heat addition to quarter of the mold sides. These cases are illustrated schematically in Fig. 2.

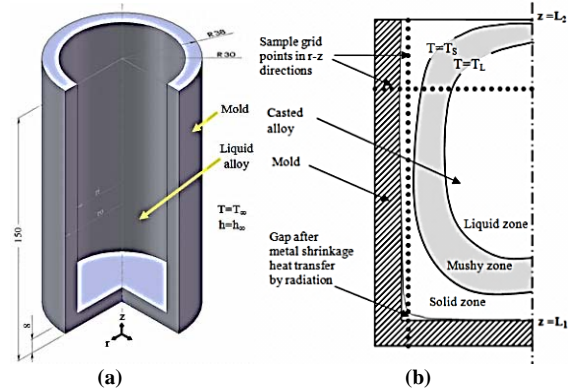


Fig. 1. Schematic diagram of the cylindrical mold (a) Cross section of three dimensional model (b) Computational domain and alloy state during solidification (All dimensions are in mm).

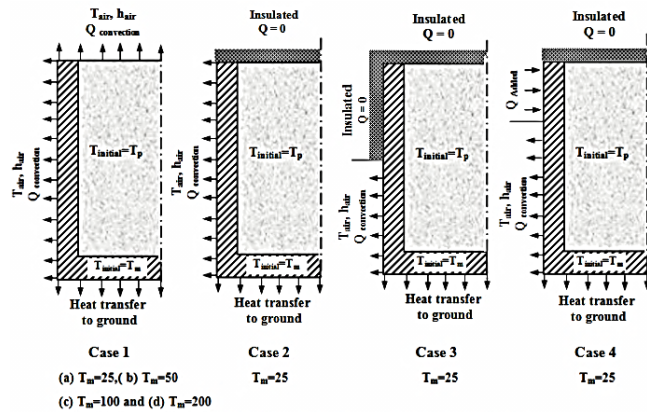


Fig. 2. The Boundary conditions for all studied cases.

## 2. Theory and Modeling

After pouring the molten metal in the mold cavity, it dissipates heat through the mold wall to the surrounding atmosphere. The solidification starts layer by layer such as the onions crust starting from the mold wall towards its center. As mentioned previously, solidification and melting processes are accompanied by phase change of the metal, which is governed by the continuity, momentum and energy equations. Since the mold filling time is small and the liquid metal has a high viscosity, the solidification problem can be considered to start at the end of the mold filling process. Therefore the governing equation becomes energy equation with heat generation [13], [14]:

$$\rho C \frac{\partial T}{\partial t} = \nabla \cdot (k \cdot \nabla T) + \dot{q} \quad (1)$$

In this expression, ( $\dot{q}$ ) is the rate of heat generated per unit volume and represents the latent heat released during the solidification process. It can be represented as [12], [15]:

$$\dot{q} = \rho L_f \frac{\partial f_s}{\partial t} \quad (2)$$

where ( $f_s$ ) is the solid metal fraction and ( $L_f$ ) is the latent heat of solidification.

Using cylindrical coordinates for axi-symmetric geometry about  $\theta$ -direction as shown in Fig.1, Eq. (1) can be rewritten as:

$$\rho C \frac{\partial T}{\partial t} = \frac{1}{r} \frac{\partial}{\partial r} \left( r k \frac{\partial T}{\partial r} \right) + \frac{\partial}{\partial z} \left( k \frac{\partial T}{\partial z} \right) + \dot{q} \quad (3)$$

By combining Eqs. (2) and (3) with constant properties, the following equation is obtained:

$$\rho C \frac{\partial T}{\partial t} = k \left[ \frac{1}{r} \frac{\partial T}{\partial r} + \frac{\partial^2 T}{\partial r^2} + \frac{\partial^2 T}{\partial z^2} \right] + \rho L_f \frac{\partial f_s}{\partial t} \quad (4)$$

The value of the specific heat depends on the situation of the metal state and can be evaluated as [16]:

$$C = \begin{cases} C_L & T \geq T_L \\ C_L f_L + C_s f_s & T_s \leq T \leq T_L \\ C_s & T \leq T_s \end{cases} \quad (5)$$

$$f_L = 1 - f_s \quad (6)$$

Where  $f_L$  is the liquid metal fraction,  $f_s$  is the frozen part in the solution depends on temperature and can be calculated using two models. The first model imposes a thermodynamic equilibrium and  $f_s$  is calculated from [17]:

$$f_s = \frac{T_L - T}{T_L - T_s} \quad (7)$$

The second model imposes non equilibrium thermodynamic and it is closer to the actual state. The second model uses the Scheil's equation to calculate  $f_s$  [16], [18]:

$$f_s = 1 - \left[ \frac{T_f - T}{T_f - T_L} \right]^{1/(k_0 - 1)} \quad (8)$$

where  $T_f$  is the melting temperature of pure metal in the cast and  $k_0$  is known as the partition coefficient, which is the ratio of solute concentration in the liquid phase to the concentration in the frozen solid solution. Eqs. (7) and (8) represent the variation of frozen solid solution with temperature. The solid metal fraction  $f_s$  in Eq. (3) can be written in terms of temperature change instead of time change using Chine Rule as follows:

$$\rho \left( C - L_f \frac{\partial f_s}{\partial T} \right) \frac{\partial T}{\partial t} = k \left[ \frac{1}{r} \frac{\partial T}{\partial r} + \frac{\partial^2 T}{\partial r^2} + \frac{\partial^2 T}{\partial z^2} \right] \quad (9)$$

The value of  $\partial f_s / \partial t$  is calculated from eq (7) or (8). The effective specific heat  $C_{ef}$  is expressed as [19]:

$$C_{ef} = \rho \left( C - L_f \frac{\partial f_s}{\partial T} \right) \quad (10)$$

The final equation in the cast metal region can be rewritten as:

$$C_{ef} \frac{\partial T}{\partial t} = k \left[ \frac{1}{r} \frac{\partial T}{\partial r} + \frac{\partial^2 T}{\partial r^2} + \frac{\partial^2 T}{\partial z^2} \right] \quad (11)$$

For the mold, the energy equation is:

$$(\rho C)_m \frac{\partial T}{\partial t} = k_m \left[ \frac{1}{r} \frac{\partial T}{\partial r} + \frac{\partial^2 T}{\partial r^2} + \frac{\partial^2 T}{\partial z^2} \right] \quad (12)$$

Where  $\rho$ ,  $C$ , and  $k$  are properties of mold material.

### 3. Initial and boundary conditions

The heat transfer through molten metal takes place by conduction. A thermal resistance is resulted at the contact between molten material outer surface and the mold wall, and it can be modeled by a coefficient  $h_{cont}$  similar to the convection heat transfer coefficient [5-8]. When the solidification starts, the frozen metal shrinks and the contact between the mold and the frozen metal skin decreases until an air gap is formed between them. At this time, heat transfer from the outer surface of molten material and the mold takes place by radiation and conduction through gases of the air gap. After testing many boundary conditions the more useful boundary conditions are formulated as follows, which are illustrated in Fig. 2 for all cases:

1) For all cases at the inner surface of the mold wall ( $r = r_i$ ) and  $z = L_1$  to  $L_2$  :

a) If the alloy is in molten state ( $T > T_s$ ) (Heat transfer through the contact)

$$-k \frac{\partial T}{\partial r} \Big|_{r=r_i} = h_{cont} (T - T_m)$$

b) If the alloy is in solid state ( $T \leq T_s$ ) (Heat transfer takes place by radiation)

$$-k \frac{\partial T}{\partial r} \Big|_{r=r_i} = \sigma \varepsilon (T^4 - T_m^4)$$

2) For all cases at the inner surface of the mold base ( $z = L_1$ ) and  $r = 0$  to  $r_i$

a) If the alloy is in molten state ( $T > T_s$ ):

$$-k \frac{\partial T}{\partial z} \Big|_{z=L_1} = h_{cont} (T - T_m)$$

b) If the alloy is in solid state ( $T \leq T_s$ ):

$$-k \frac{\partial T}{\partial z} \Big|_{z=L_1} = \sigma \varepsilon (T^4 - T_m^4)$$

3) For all cases at the outer surface of the mold base ( $z = 0$ ) and  $r = 0$  to  $r_o$

$$-k \frac{\partial T}{\partial z} \Big|_{z=L_1} = h_{cont} (T_m - T_{gr})$$

4) At the outer surface of the mold ( $r = r_o$ )

- a) Case1 and case2, whole surface subjected to convection  $z = 0$  to  $L_2$

$$-k \frac{\partial T}{\partial r} \Big|_{r=r_o} = h_{\infty}(T_m - T_{\infty})$$

- b) Case3, the lower half of the surface subjected to convection while the rest half is insulated

$$-k \frac{\partial T}{\partial r} \Big|_{r=r_o} = h_{\infty}(T_m - T_{\infty}) \quad \text{for } z = 0 \text{ to } L_2/2$$

$$q = 0 \quad \text{for } z = L_2/2 \text{ to } L_2).$$

- c) Case 4, three fourth of the surface subjected to convection while heat is added to the reminder surface

$$-k \frac{\partial T}{\partial r} \Big|_{r=r_o} = h_{\infty}(T_m - T_{\infty}) \quad \text{for } z = 0 \text{ to } 3/4 L_2$$

$$q = q_{add} \quad \text{for } z = 3/4 L_2 \text{ to } L_2$$

- 5) At the top surface of the mold and the molten material

- a) Case1, heat transfer by convection from the top

- i) At the molten metal surface ( $r = 0$  to  $r_i$ )

$$-k \frac{\partial T}{\partial z} \Big|_{z=L_2} = h_{\infty}(T_{alloy} - T_{\infty})$$

- ii) At the mold surface ( $r = r_i$  to  $r_o$ )

$$-k \frac{\partial T}{\partial z} \Big|_{z=L_2} = h_{\infty}(T_m - T_{\infty})$$

- b) Case2, case3 and case4, the mold is insulated at the top surface

$$q = 0$$

- 6) Because of the symmetry around the axial direction, one half of the domain was analyzed. Hence the boundary condition at the center is:

$$\frac{\partial T}{\partial r} = 0 \quad \text{at } r = 0$$

For the initial conditions, it is assumed that the filling time is very small and the temperature distribution is homogeneous throughout the molten metal at the filling end and it is equal the pouring temperature. Thus, the initial alloy temperature is:  $T_{initial} = T_p = 700$  °C.

The initial mold temperature for case1 (1a, 1b, 1c and 1d) are taken to be 25, 50, 100 and 200 °C respectively. The mold temperature is fixed at 25 °C for cases 2, 3 and 4. The thermo-physical properties used in the simulation are summarized in Table 1.

**Table 1: Thermo-physical properties used in the simulation [13][14][15]**

Thermo-physical properties of the casted alloy	
thermal conductivity– solid phase	193 W/m K
thermal conductivity– liquid phase	89 W/m K
specific heat– solid phase	1090 J/kg K
specific heat– liquid phase	1052 J/kg K
density– solid phase	2654 Kg/m <sup>3</sup>
density– liquid phase	2488 Kg/m <sup>3</sup>
solid temperature	561 °C
liquid temperature	646 °C
latent heat in melting	394,000 J/kg
equilibrium partition coefficient	0.14
Thermo-physical properties of the mold	
thermal conductivity	33.5 W/m K
specific heat	628 J/kg K
Density	7210 Kg/m <sup>3</sup>
Other data	
heat transfer coefficient metal–mold interface, $h_{cont}$	1050 W/m <sup>2</sup> .K
convection heat transfer coefficient to the air, $h_{\infty}$	83 W/m <sup>2</sup> .K
Emissivity of the molten material	0.25

#### 4. Numerical solution and code validation

The governing equations for transient temperature distribution within the cast and the mold wall are Eqs. (11) and (12), respectively. Equation (12) can be solved using marching technique without difficulty because of the linearity nature. However, Eq. (11) contains a nonlinear term ( $\partial f_s / \partial T$ ) embedded in  $C_{ef}$  equation that must be linearized. One of the methods used to linearize this equation is the explicit calculation of the nonlinear term. Equations (11) and (12) are solved using explicit finite difference method starting from initial condition until all metal solidifies in the mold [20]. The metal solidification happens when the ingot temperature in all grid points are equal or less than  $T_s$ .

As shown in Fig.1, the solution domain is a cylindrical mold with dimensions of 150 mm height, 38 mm outer radius, and wall thickness of 8 mm filled with molten metal. The solution domain is divided into 1 mm×1 mm grid to increase the solution accuracy. The numbers of divisions are 38 nods in  $r$ -direction (30 divisions in the ingot region and 8 divisions in the mold wall) and 150 nods in the  $z$ -direction (142 divisions in the ingot region and 8 divisions in the mold wall). To attain stability condition for explicit method and increase the solution accuracy, a time step size of  $\Delta t = 2.5 \times 10^{-3}$  s is used (400 time-step represents one second).

A FORTRAN-90 program was used to write the code and solving equations 8, 10, 11 and 12 to find the temperature distribution in both the mold wall and the casted metal with the specified boundary conditions. The flow chart of FORTRAN code is shown in Fig.3. The program consists of three main parts, namely: mesh generation, specification of initial and boundary conditions, and solutions of governing equations to get the field variable  $T$  at all grid points in the solution domain and printout the results.

The model validation is an essential part of the numerical investigation. Validation of the present computer program results are carried out with the results of Ehlen et al [21]. An Al-7wt%Si alloy was poured into a cylindrical cast iron chill mold  $H=107$  mm,  $R=40$  mm. Fig. 4 shows the distribution of computed temperature after 30 and 80 sec, respectively. The results showed a good agreement for temperature distribution at these two states.

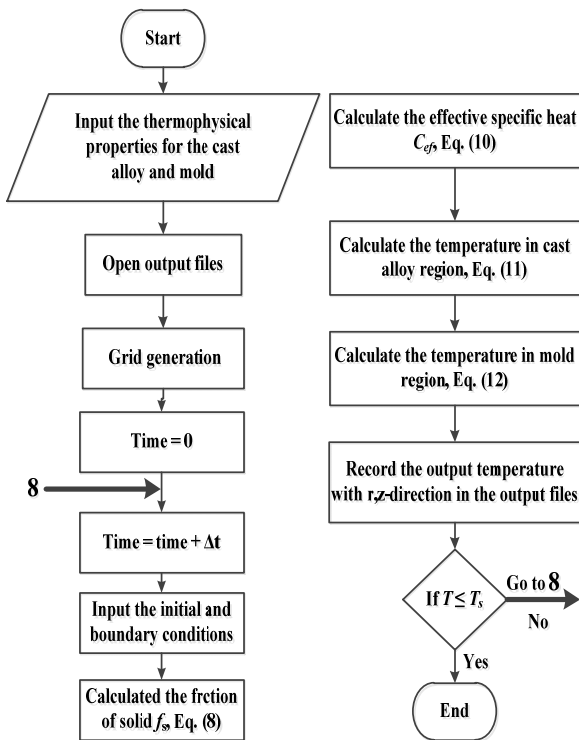


Fig. 3. Flow chart of the FORTRAN code.

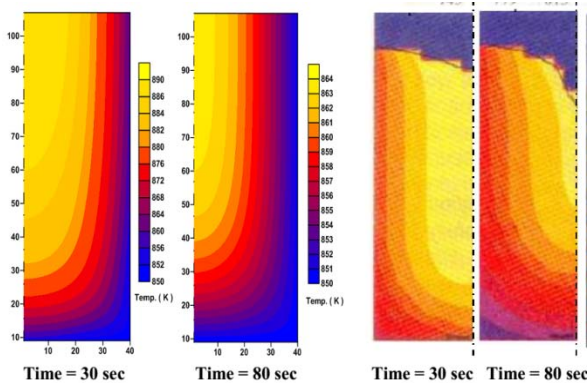


Fig. 4. Comparison the temperature distribution of the present results with previous work by Ehlen et al [21]

## 5. Results and discussion

The effect of solidification mode on the primary and secondary cavities of Al-4.5 wt.%Cu alloy cast in a cylindrical mold was numerically studied. The solidification mode was investigated under four major different cases: Case (1): solidification without applying any effect on the mold for four different initial mold temperature (case1-a,  $T_m=25$ , case1-b,  $T_m=50$ , case1-c;  $T_m=100$ , case1-d;  $T_m=200$ ), Case (2): mold top is insulated, Case (3): thermal insulation of the upper half of the mold sides and Case (4): heating the upper quarter of the mold sides. The results were represented in terms of temperature distribution within the ingot at deferent time level.

### 5.1 Effect of the mold temperature ( case1)

The molten metal was poured from 700 °C into the mold. The mold temperature was 25 °C. Figure 6 reveals the temperature distribution of the cast metal from the end of pouring to the end of solidification. The mushy zone between the liquid temperature  $T_L$  and the solid temperature  $T_S$  is shaded with a gray color to illustrate the progress of the solidification process. From the temperature distribution contours, three solidification directions are observed. The first is an axial upward direction, which is caused by the mold base that works as a heat sink and dissipates the heat to the surrounding. The second is an axial downward direction due to heat transfer by radiation at the upper surface of the ingot, which is exposed to the surrounding atmosphere. The third direction is in the radial direction due to the heat dissipation from mold side to the atmosphere. This mode of solidification leads to an ingot with a last solidification metal to be the mid-height zone of the mold. This isolated pasty metal zone shrinkage on solidification and as no feeding metal cannot reach this zone, sever shrinkage porosity or even secondary cavity can appear.

Figures 7 to 9 in addition to Fig. 6 show the effect of the mold temperature on the solidification mode and temperature distribution within the solidified metal. It can be observed from these figures, that rising mold temperature from 25 to 200 °C has almost no significant effect on temperature distribution and major solidification direction. However, the only effect of this parameter is increasing the solidification period, which is clear from these figures when comparing the time for approximately same temperature distribution at the last stage of solidification (77s, 82s, 91s and 120s) that can coarsen the produced microstructure.

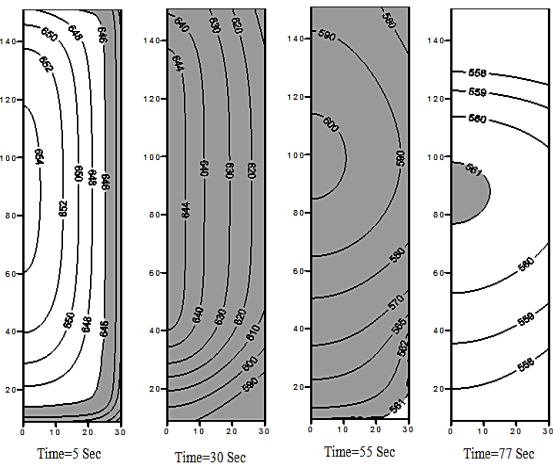


Fig. 6. Temperature distribution of alloy casted in a mold at 25 °C with heat transfer from the top case 1-a

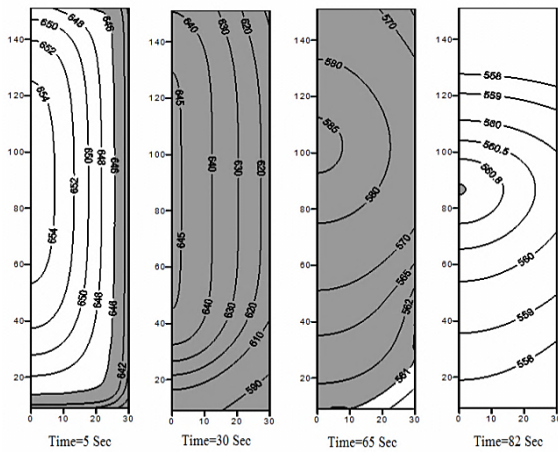


Fig. 7. Temperature distribution of alloy casted in a mold at 50 °C with heat transfer from the top case 1-b.

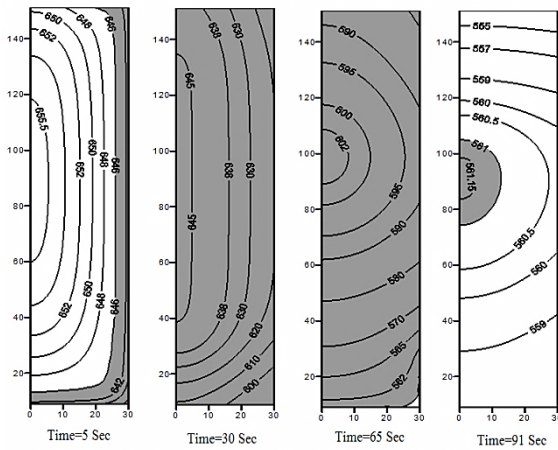


Fig. 8. Temperature distribution of alloy casted in a mold at 100 °C with heat transfer from the top case 1-c.

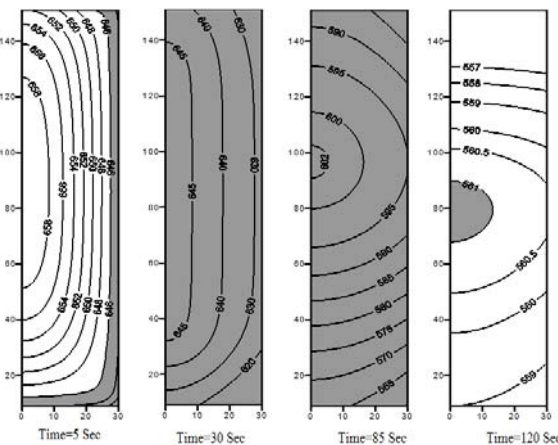


Fig. 9. Temperature distribution of alloy casted in a mold at 200 °C with heat transfer from the top case 1-d.

### 5.2 Effect of thermal insulation of the mold top case 2

The temperature distribution for a metal solidified a mold at 25°C with insulation at its top is represented in Fig. 10. It is observed that only two major solidification directions are present: axial direction from the bottom to the top (upward direction) and radial direction from the ingot outer surface to the

center. The third downward solidification direction that was noted previously for non-insulated mold disappeared due to the top insulation. This situation had approximately radial upward solidification, which makes the ingot top to be the last solidification portion and shifts all solidification shrinkage to the ingot top and changes it to a primary cavity. This solidification mode makes the hot spots and the accompanied secondary cavity to disappear. This is a preferred solidification mode.

### 5.3 Effect of insulation of mold upper portion case 3

Figure 11 illustrates the temperature distribution of an ingot poured into a mold insulated from the upper half to delay metal solidification at this portion of the ingot. The solidification in this case is without any hot spots or secondary cavity. Only a primary cavity will appear at the top of the ingot, where all shrinkage takes place. It is observed that the solidification direction are exactly similar to that was observed in case 2 with the exception that the ratio of the depth Y to the width X is smaller for this case than case 2, this mean smaller primary cavity depth and more benefit high of the ingot.

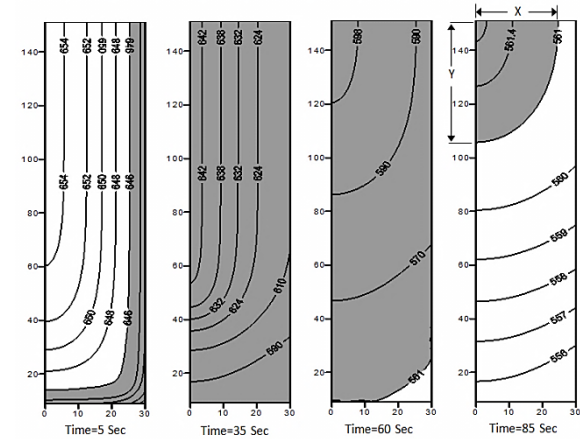


Fig. 10. Temperature distribution of alloy casted in a mold at 25 °C isolated at the top.

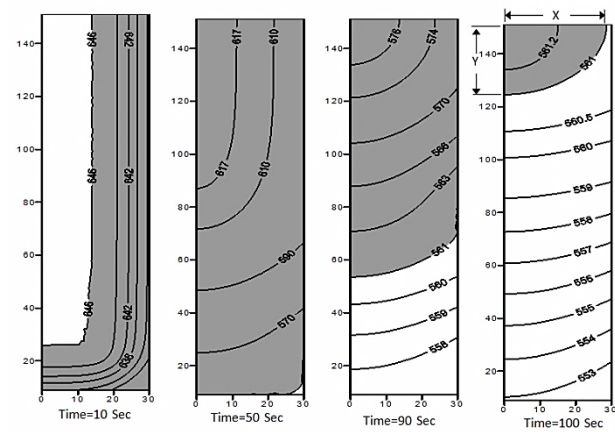


Fig. 11. Temperature distribution of alloy casted in a mold at 25 °C insulated at the top and the half of its height.

### 5.4 Effect of adding heat to the upper portion of the mold (case 4)

Another method can be used to satisfy unidirectional solidification from the bottom toward the top. This method is represented by adding heat source at the upper quarter of the mold to compensate the heat lost by radiation and convection at the mold top and conduction at the mold wall. This situation is

clearly observed in Fig. 12. At early stages of solidification (to about 60s), similar temperature distribution within the solidification metal was observed in Figs. 10, 11 and 12. But with progress in solidification process, the solidification surface becomes more flatten in contrast to concave up shape in previous cases. In the final stage where the solidification completes the surface become horizontal. As a result the secondary cavity will also vanish in addition to the primary cavity and hot spots. This case is considered to be the best case improving the maximum yield of ingot height.

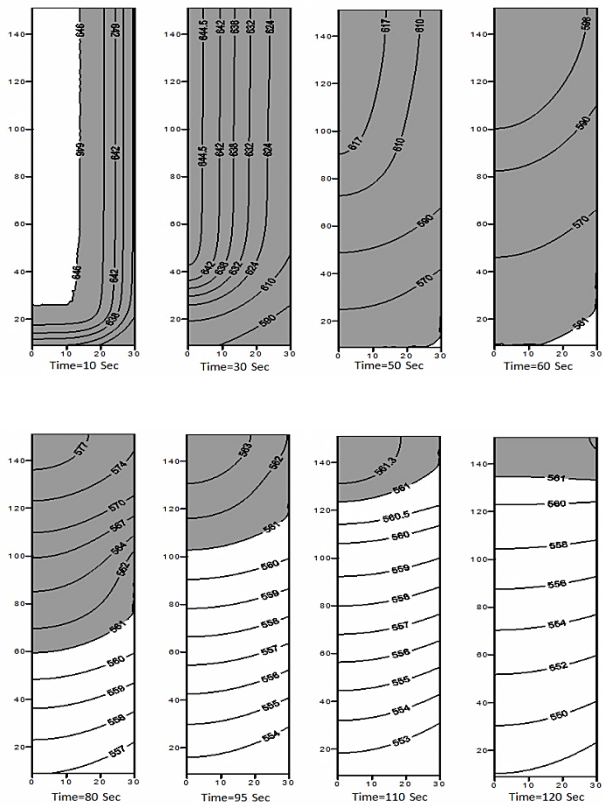


Fig. 12. Temperature distribution of alloy casted in a mold at 25 °C isolated at the top and heat added to quarter of its height

## 6. Conclusions

The effects of the solidification configuration on the primary and secondary cavities to specify the optimum solidification conditions for aluminum-copper Al 4.5 wt.%Cu alloy casted in a cylindrical mold was numerically studied. According to the obtained results, the key conclusions can be drawn:

- Increasing the mold temperature leads to increase the solidification time only while it has a little effect on the temperature distribution during the solidification and the final cast shape.
- The thermal insulation of the mold top moves the last solidification region to the top of the cast leading to get an ingot rid of the secondary cavity.
- The thermal insulation of a portion of the upper wall of the mold makes the cast surface to be more homogeneous and reduces the secondary cavity size.

- The heat addition to a portion of the upper wall of the mold for a specific time leads to obtain a cast with approximately flat surface hence free from secondary cavity in addition to primary cavity.
- The solidification time can be increased by increasing the mold temperature, by insulating the mold, or by adding heat to the mold wall.

## Nomenclature

A	area, m <sup>2</sup>
C	specific heat, J/(Kg K)
f	metal fraction
k	thermal conductivity, W/(m K)
k <sub>0</sub>	the equilibrium partition coefficient
L	ingot height, m
L <sub>f</sub>	solidification latent heat, J/kg
h	heat transfer coefficient, W/(m <sup>2</sup> K)
r	radial variable (radius)
t	solidification time, sec
T	temperature, °C
z	spatial variable

### Greek symbols

ρ	density, kg/m <sup>3</sup>
ε	thermal emissivity
σ	Stefan–Boltzmann constant

### Subscripts

ef	effective
i	inner
L	liquid phase
m	Mold
p	Pouring
s	solid phase
∞	ambient, air

## References

[1] Ali, A., & Emad, S. (2003). Study of heat transfer and flow of molten metal in molds plumbing minute. *The Iraqi Journal of Mechanical Engineering and Materials Engineering*, 1(3), 20–26.

[2] Stefanescu, D.M. (2009). *Science and engineering of casting solidification*. USA: Springer Science & Business Media, LLC.

[3] Singh, A.K., Pardeshi, R., & Basu, B. (2001). Modelling of convection during solidification of metal and alloys, *Sadhana*, 26(1–2), 139–162.

- [4] Walker, J. S., & Georgopoulos, E. (1984). Slow solidification of a cylinder with constant heat efflux. *International Communications in Heat and Mass Transfer*, 11, 45–53.
- [5] Ferreira, I. L., Spinelli, J. E., Pires, J. C., & Garcia, A. (2005). The effect of melt temperature profile on the transient metal/mold heat transfer coefficient during solidification. *Materials Science and Engineering A*, 408(1), 317–325.
- [6] Bertelli, F., Brito, C., Meza, E.S., Cheung, N. & Garcia, A. (2012). Inward and outward solidification of cylindrical castings: the role of the metal/mold heat transfer coefficient. *Materials Chemistry and Physics*, 135(1–2), 545–554.
- [7] Santos, C.A., Siqueira, C.A., Garcia, A., Quaresma, J.M.V., & Spim, J.A. (2004). Metal-mold heat transfer coefficients during horizontal and vertical unsteady-state solidification of Al-Cu and Sn-Pb alloys. *Inverse Problems in Science and Engineering*, 12(3), 279–296.
- [8] Silva, J.N., Moutinho, D.J., Moreira, A.L., Ferreira, I.L., & Rocha, O.L. (2011). Determination of heat transfer coefficients at metal–mold interface during horizontal unsteady-state directional solidification of Sn-Pb alloys. *Materials Chemistry and Physics*, 130(1), 179–185.
- [9] Spinelli, J.E., Cheung, N., Goulart, P.R., Quaresma, J., & Garcia, A. (2012). Design of mechanical properties of Al-alloys chill castings based on the metal/mold interfacial heat transfer coefficient. *International Journal of Thermal Sciences*, 51, 145–154.
- [10] Bermúdez, A., & Otero, M.V. (2004). Numerical solution of a three-dimensional solidification problem in aluminum casting. *Finite Elements in Analysis and Design*, 40(13–14), 1885–1906.
- [11] Abbas Nejad, A., Maghrebi, M.J., Basirat Tabrizi, H., Heng, Y., Mhamdi, A., & Marquardt, W. (2010). Optimal operation of alloy material in solidification processes with inverse heat transfer. *International Communications in Heat and Mass Transfer*, 37(6), 711–716.
- [12] Shi, Z., & Guo, Z.X. (2004). Numerical heat transfer modelling for wire casting. *Materials Science and Engineering A*, 365(1–2), 311–317.
- [13] Kulkarni, S.N., & Radhakrishna, K. (2007). Prediction of solidification time during solidification of aluminum base alloy castings cast in CO<sub>2</sub>-sand mold. *The International Journal of Advanced Manufacturing Technology*, 34(11–12), 1098–1110.
- [14] Holman, J.P. (2010). *Heat transfer*, Tenth ed., New York, USA: McGraw-Hill Companies, Inc.
- [15] Melo, M.d.L.N.M., Rizzo, E.M.S., & Santos, R.G. (2004). Numerical model to predict the position, amount and size of microporosity formation in Al-Cu alloys by dissolved gas and solidification shrinkage. *Materials Science and Engineering A*, 374(1–2), 351–361.
- [16] Jafari, A., Seyedein, S.H., & Haghpanahi, M. (2008). Modeling of heat transfer and solidification of droplet/substrate in micro-casting SDM process. *IUST International Journal of Engineering Science*, 19, 187–198.
- [17] Shabani, M.O., & Mazahery, A. (2011). Application of finite element method for simulation of mechanical properties in A356 alloy. *International Journal of Applied Mathematics*, 7, 89–97.
- [18] Tambunam, B. (2005). *Simulation of heat transfer solidification with improved latent heat parameter in continuous casting*, in: Seminar National MIPA–2005, FMIPA–Universitas Indonesia Depok: Indonesia,.
- [19] Santos, C.A., Quaresma, J.M.V., & Garcia, A. (2001). Determination of transient interfacial heat transfer coefficients in chill mold castings. *Journal of Alloys and Compounds*, 319(1), 174–186.
- [20] Patankar, S.V. (1980). *Numerical heat transfer and fluid flow*. USA: Hemisphere, Washington, DC.
- [21] Hansen, P.N., Conley, J.G. (Eds.) *IX International Conference on Modeling of Casting, Welding and Advance Solidification Process*. TMS, pp. 633–639.